# Experimental and Theoretical Investigation of Interaction Effect on Energy Absorption of Bi-tubular Structures Under Quasi-static Axial Crushing


**K. Vinayagar, A. Senthil Kumar, M. Vel Vignesh, and K. Gokulan**

**Abstract** This work reveals the interaction effect on energy absorption of bi-tubular, a combination of outer circular tube with inner polygonal tube structures under quasi-static axial crushing. First, the experimental mean crushing force of single tubes was compared with theoretical prediction, and it witnesses good agreement between them. In bi-tubular arrangement, the inscribed diameter of inner polygonal tubes plays an important role in improving the mean crushing force by interaction effect. The mean crushing force of bi-tubular specimens D3T, D3S, and D3H has 35, 26, and 10.1% higher than the summation of their individual single tubes that is SC with S3T or S3S or S3H.

**Keywords** Bi-tubular structures · Quasi-static axial crushing · Interaction effect · Mean crush force · Specific energy absorption

## Nomenclature

| | |
|---|---|
| $D$ | Diameter of the tube, m |
| $M_o = \sigma_o h^2/4$ | Full plastic bending moment of tube wall per unit length, N |
| $m$ | Mass of the thin-walled structure, kg |
| $F_{mean}$ | Mean crushing force, N |
| $F_{Peak}$ | Peak crushing force, N |
| $C$ | Side of the polygon, m |
| $h$ or $t$ | Thickness of the tube, m |
| $\delta$ | Crushing distance or crushing deflection, m |
| $\sigma_o$ | Flow stress, N/m$^2$ |

K. Vinayagar (✉) · A. Senthil Kumar · M. Vel Vignesh · K. Gokulan
Department of Mechanical Engineering, Sethu Institute of Technology, Kariapatti, Virudhunagar, Tamil Nadu 626115, India
e-mail: k_vinayagar@ymail.com

A. Senthil Kumar
e-mail: asenthil123@yahoo.com



L.-J. Yang et al. (eds.), *Proceedings of ICDMC 2019*,
Lecture Notes in Mechanical Engineering,
https://doi.org/10.1007/978-981-15-3631-1_48

$\sigma_u$ Ultimate tensile stress, N/m$^2$
$\sigma_y$ Yield stress, N/m$^2$

## 1 Introduction

During collision, energy absorption devices are responsible to reduce the loss of life and damage of vehicle critical parts. These devices can absorb maximum kinetic energy by permanent plastic deformation and transferred minimum amount of force to occupants. From the different types of energy absorbers, the metallic thin-walled tubes are considered one of the most efficient energy-absorbing devices for their ease manufacture, high strength, and low cost [1, 2]. Over the past few decades, many researchers studied about crashworthiness of thin-walled cylinders and have submitted in experimental, analytical, and numerical results with different cross sections, materials, tubes filled with foam, and multi-cell thin-walled structures [3, 4].

The analysis of axial crushing on thin-walled cylinders was pioneered by Alexander [5], and the work yields an excellent theoretical model to access the average crushing force for axisymmetric fold pattern. Subsequently, Abramowicz and Jones [6] analyzed the different types of crushing modes and took more efforts to improve the previous theoretical models by the number of experiments on the concertina or ring mode for circular cylinders. Hong et al. [7] studied collapse mode and energy absorption of triangular tubes under quasi-static axial compression experiments. Based on folding elements, they proposed four different theoretical models to predict the mean crushing force. Abramowicz et al. [8] studied the effect of corner element of an arbitrary angle on energy absorption by using rigorous methods of structural plasticity with finite deformations and rotations. Based on this analysis, they developed mathematical models to predict the mean crushing force of multi-corner columns with an even number of corners such as square, hexagonal, and rhomboidal thin-walled columns.

Alavi Nia et al. [9, 10] and Velmurugan et al. [11, 12] explored different configurations in single material and showed that geometric parameter in a conventional way to improve the crashworthiness of thin-walled structures.

When using foam, honeycomb, or sawdust as filler materials, the energy absorption capacity of the thin-walled structures was found to be increased by interaction between them. Hanssen et al. [13–15] carried out complete studies on aluminum columns with aluminum foam filler and identified a strong foundation for the subsequent theoretical analysis and practical application. In recent years, foam-filled tubes with various cross sections such as circular [13], square [14–16], polygonal [17], and elliptical [18] have been carried out extensively.

The effect of length difference on crashworthiness performance of bi-tubal structures was reported by Sharifi et al. [19], Vinayagar et al. [20], and Kashani et al. [21]. Recently, Vinayagar et al. [22], Rahi [23], and Kamran et al. [24] were reported the influence of geometry on the energy absorption of bi-tubes under axial compression.

Though the crushing of bi-tubular systems is very recent topics in crashworthiness analysis, the discussion about interaction effect with quantitative results is very minimum. The energy absorption capabilities of single tubes with various sections were studied experimentally, and experimental results were compared with theoretical predictions [22]. Due to the interaction effect, the bi-tubular combination has higher mean crushing force, when compared with the summation of mean crushing force of individual single tubes and the percentage of improvement in mean crushing force also reported.

## 2 Definition of Crashworthiness Indicators

With the purpose of better understanding about crashworthiness of thin-walled structures, some indicators like total energy absorption (TEA), specific energy absorption (SEA), and mean crush force ($F_{\text{mean}}$) are described with a brief explanation.

**Total Energy Absorption**
Total energy absorption expresses the energy absorption capacity of specimens. It can be determined by integration of the axial crushing force versus displacement.

$$\text{TEA} = \int_0^{\delta} F(\delta)\mathrm{d}\delta \tag{1}$$

where $F(\delta)$ is the instantaneous crushing force with a function of the crushing distance $\delta$. From experiments or numerical modeling, the instantaneous crushing force can be obtained.

**Specific Energy Absorption**
Specific energy absorption is defined as energy absorbed per unit mass of the thin-walled member. It is used to compare the energy absorption capacity of structures with different mass which is given by

$$\text{SEA} = \text{TEA}/m \tag{2}$$

**Mean Crush Force**
The average crush force is also one of the response parameters for the energy absorption capability of a structure, which is calculated as,

$$F_{\text{mean}} = \text{TEA}/\delta \tag{3}$$

where TEA is energy absorbed during collapse with displacement $\delta$.

## 3 Specimen Preparation

Since the desirable tube sections were not available in the market, the specimens were prepared in sheet metal shop from 0.478 mm thick SS304 stainless steel sheet. The stainless steel sheet was cut into the required dimensions and joined as a tube by TIG welding process. Stainless steel 304 is considered for its good formability and strength. Mechanical properties of this sheet metal were presented in Table 1.

Single tubes of various polygonal sections such as triangle, square, and hexagon were fabricated according to three levels of inscribed diameter of polygonal section such as 60 mm, 70 mm, and 80 mm. The edge length of various polygonal sections is derived from the inscribed diameter of the polygonal section as shown in Fig. 1 and tabulated in Table 2. The length of all the single tubes is 135 mm.

### *3.1 Coding System of Single Tubes*

The prepared single tube specimens were coded for the purpose of easy identification, evaluation, and performance comparison. In coding of single polygonal tubes, the first alphabet 'S' indicates single tube and the second numerical number 1, 2, and 3 indicates the level of inscribed diameter of the polygonal section, i.e., 60 mm, 70 mm, and 80 mm, respectively; then, the third alphabet indicates section of tube, i.e., *T* for triangular, *S* for square, and *H* for hexagonal section. The coding method of single tubes is noted in Table 3.

For example, S2H means single tube with 70 mm (second level) inscribed diameter of the polygonal section, and its section was a hexagon. Then, the circular cylinder was fabricated with a diameter of 90 mm. The single cylinder was coded as SC, here also '*S*' stands for single and '*C*' stands for cylinder. For consistency of output in each type of geometry, three samples were fabricated.

### *3.2 Experimental Process*

For this quasi-static axial compression analysis, FSA makes Model TUF-CN 1000 servo controlled universal testing machine (Fig. 2) was used. The samples were crushed at a loading rate of 10 mm/min as previous study [22]. Here also, the specimens were crushed up to 100 mm at the room temperature of 25 °C.

**Table 1** Mechanical properties of 304 stainless steel sheet

| Property | Ultimate tensile strength (MPa) | Yield stress (MPa) | % of elongation |
|---|---|---|---|
| Value | 531.2 | 223.6 | 41 |

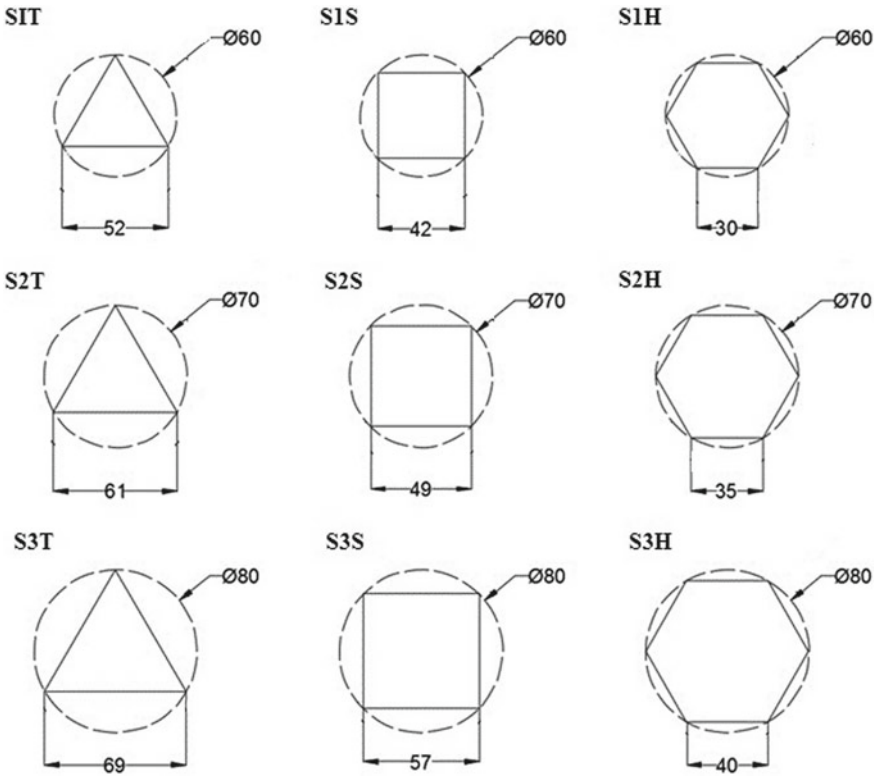


**Fig. 1** Section geometry and dimensions of single tube specimens (all dimensions are in mm)

**Table 2** Specifications of single tubes

| S. No. | Code | Inscribed diameter of the polygonal section (mm) | Section of the tube | Side/edge length of polygon (mm) |
|---|---|---|---|---|
| 1 | S1T | 60 | Triangle | 52 |
| 2 | S1S | 60 | Square | 42 |
| 3 | S1H | 60 | Hexagon | 30 |
| 4 | S2T | 70 | Triangle | 61 |
| 5 | S2S | 70 | Square | 49 |
| 6 | S2H | 70 | Hexagon | 35 |
| 7 | S3T | 80 | Triangle | 69 |
| 8 | S3S | 80 | Square | 57 |
| 9 | S3H | 80 | Hexagon | 40 |
| 10 | SC | 90 | Cylinder | Ø 90 |

**Table 3** Coding system of single tubes

| Coding order | Code | Description |
|---|---|---|
| First alphabet | S | Single tube |
| Second numerical number | 1 | Inscribed diameter of polygonal section is 60 mm |
| | 2 | Inscribed diameter of polygonal section is 70 mm |
| | 3 | Inscribed diameter of polygonal section is 80 mm |
| Third alphabet | T | Polygonal section of tube is triangle |
| | S | Polygonal section of tube is square |
| | H | Polygonal section of tube is hexagon |

**Fig. 2** Computerized servo controlled universal testing machine

## 4 Results and Discussion

Load–displacement curves of the single tube specimens are obtained from quasi-static tests. The important crashworthiness parameters such as mean crushing force, total energy absorption, and specific energy absorption were calculated from the load–displacement curves of the single tube specimens and recorded in Table 4.

Concertina mode is developed in specimen SC; in-extensional mode is developed in single polygonal tubes; and diamond mode is observed in all bi-tubular specimens. Based on experimental results, a detailed comparison report of the crashworthiness performance between various polygonal sections in three levels of inscribed diameter of single tubes was presented.

**Table 4** Experimental results of single tubes

| Specimen code | Mass (kg) | $F_{mean}$(kN) | $F_{Peak}$(kN) | TEA (J) | SEA (kJ/kg) | CFE (%) |
|---|---|---|---|---|---|---|
| SC | 0.140 | 8.18 | 16.08 | 820.7 | 5.862 | 50.87 |
| S1T | 0.080 | 2.81 | 5.57 | 281.3 | 3.516 | 50.45 |
| S1S | 0.083 | 4.45 | 8.11 | 458.8 | 5.528 | 54.87 |
| S1H | 0.090 | 6.10 | 11.59 | 611.1 | 6.790 | 52.63 |
| S2T | 0.095 | 3.11 | 5.78 | 318.9 | 3.357 | 53.81 |
| S2S | 0.100 | 4.62 | 8.54 | 475.6 | 4.756 | 54.10 |
| S2H | 0.103 | 6.96 | 12.56 | 698.4 | 6.780 | 55.41 |
| S3T | 0.105 | 3.25 | 5.95 | 325.8 | 3.103 | 54.62 |
| S3S | 0.115 | 4.88 | 8.96 | 491.8 | 4.277 | 54.46 |
| S3H | 0.120 | 7.55 | 15.18 | 758.6 | 6.322 | 49.74 |

## *4.1 Effect of Inscribed Diameter on Mean Crushing Force of Single Tubes*

On crashworthiness, the effect of the inscribed diameter of polygonal section of single tubes is studied. The edge length of polygon is increased with the inscribed diameter of polygonal section from 60 mm, 70 mm, and 80 mm. When the area of polygonal sections is increased, the stability of tubes also increased. This is the main reason for improvement of energy absorption capability. Mean crushing force of tested sections for various inscribed diameters of polygonal sections is compared in Fig. 3. It can be understood from this diagram for the same section of single tube, mean crushing force increased with increasing of the inscribed diameter of polygonal section. As in Table 4, the total energy absorption of the thin-walled tubular structures with inscribed diameter of polygonal section of 60 mm, 70 mm, and 80 mm is the least, medium, and the most, respectively.

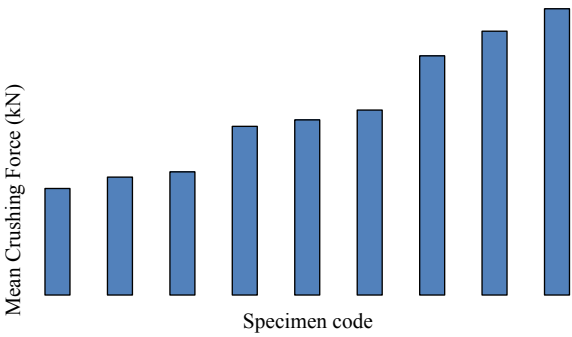


**Fig. 3** Effect of inscribed diameter of polygonal section on mean crushing force of single tubes

### 4.2 *Effect of Polygonal Section of Single Tube*

Thin-walled structures are used to dissipate the impact energy through the process of plastic deformation. In fact, the studies [9, 10] have shown that the amount of absorbed energy increased with the number of sides of a section. The reason for this is the number of plastic hinges and folds which are increased with number of sides of polygon. Figure 4 shows the comparisons of mean crushing force between various sections of tubes for a particular inscribed diameter of the polygon. Figure 4 also pointed out that the mean crushing force increased by increasing the number of edges or corners of the section of any of inscribed diameter of the polygonal section.

From Table 4, TEA of hexagonal tube was greater than the square and the square was greater than the triangle; i.e., in anyone of inscribed diameter of the polygonal section, the greater the number of sides, the absorbed energy is more. The hexagonal tubes have more SEA than the other sections as presented in Table 4 and it is shown in Fig. 5.

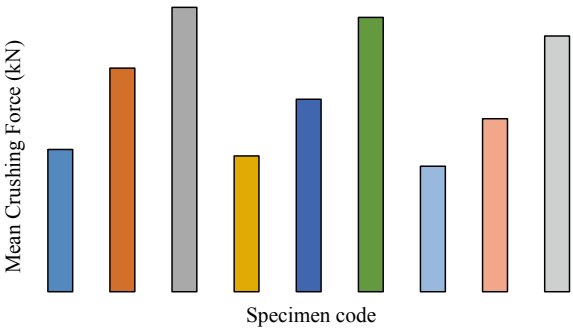


**Fig. 4** Effect of polygonal section on mean crushing force of single tubes

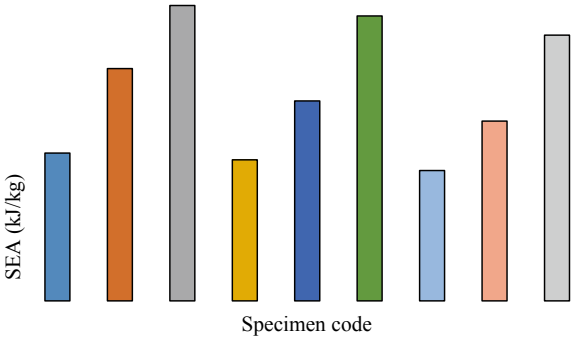


**Fig. 5** Effect of polygonal section on SEA of single tubes

### *4.3 Theoretical Predictions*

Comparison of experimental results with theoretical predictions was a must to validate the experiments. To predict the mean crushing force of single tubes, several theoretical models have been addressed by many researchers for concertina and diamond mode of various sectional tubes such as circular, triangle, square, and hexagon.

**Theoretical Model of Circular Cylinder**
The important expression of mean crushing force for concertina mode of circular cylinder is derived by Abramowicz and Jones [6] in 1984.

$$F_{\text{mean}} = \frac{20.79\left(\frac{D}{t}\right)^{0.5} + 11.9}{0.86 - 0.568\left(\frac{t}{D}\right)^{0.5}} M_o \tag{4}$$

**Theoretical Model of Triangular Tube**
For triangular tube, Hong et al. [7] presented the following model for the mean crushing force which is,

$$F_{\text{mean}} = 26.66 M_o \left(\frac{C}{t}\right)^{\frac{1}{3}} \tag{5}$$

**Theoretical Model of Square Tube**
The following classic theoretical model for square tube under axial compression was proposed by Abramowicz and Wierzbicki [8],

$$F_{\text{mean}} = 12.16 \sigma_o C^{0.37} t^{1.63} \tag{6}$$

Most of the experimental studies were validated based on this theoretical model.

**Theoretical Model of Hexagonal Tube**
The theoretical expression presented by Abramowicz and Wierzbicki [8] for hexagonal column is approximated by the following functions,

$$F_{\text{mean}} = 20.2 \sigma_o C^{0.4} t^{1.6} \tag{7}$$

**Determination of Flow Stress**
Actually, flow stress is not a constant value, so determination of the flow stress is very important. During loading, the strains for different collapse modes and in different regions of tubes are different. Therefore, different expressions were employed by the researchers to calculate the flow stress. In this present work, the average value of yield stress and ultimate tensile stress is employed as flow stress for all of the thin-walled structures.

Based on the above mathematical Eqs. (4–7), the theoretical mean crushing force was calculated for all sections of tubes. Then, the values of experimental mean crushing forces of single tubes for circular, triangular, square, and hexagonal sections are

**Table 5** Experimental results versus theoretical predictions of single tubes

| Specimen code | Mean crushing force (kN) | | Percentage of deviation |
|---|---|---|---|
| | Experimental result | Theoretical prediction | |
| SC | 8.18 | 7.8 | 4.8 |
| S1T | 2.81 | 2.7 | 4.0 |
| S2T | 3.11 | 2.9 | 7.2 |
| S3T | 3.25 | 3.01 | 7.9 |
| S1S | 4.45 | 4.3 | 3.5 |
| S2S | 4.62 | 4.53 | 2.0 |
| S3S | 4.88 | 4.74 | 3.0 |
| S1H | 6.1 | 6.5 | 6.6 |
| S2H | 6.96 | 6.8 | 2.4 |
| S3H | 7.55 | 7.3 | 3.4 |

compared with theoretically predicted values in Table 5. From Table 5, the percentage of deviation is very less and it can be understood that the theoretical predictions are found to be in a good agreement with the experimental results.

## *4.4 Comparison Between Single and Bi-tubular Structures*

Experimental results of crashworthiness indicators for bi-tubular structures are taken from the previous work [22] and tabulated in Table 6. Table 6 shows that the mean crushing force, total energy absorption, and specific energy absorption of the bi-tubes were greater than the single tubes.

**Table 6** Experimental results of bi-tubes

| Code | Mass (kg) | $F_{\text{Peak}}$ (kN) | $F_{\text{mean}}$ (kN) | TEA (J) | SEA (kJ/kg) |
|---|---|---|---|---|---|
| D1T | 0.220 | 21.80 | 10.76 | 1081.8 | 4.917 |
| D1S | 0.223 | 24.12 | 12.59 | 1265.7 | 5.676 |
| D1H | 0.230 | 29.13 | 14.57 | 1459.5 | 6.346 |
| D2T | 0.235 | 22.85 | 12.11 | 1227.7 | 5.224 |
| D2S | 0.240 | 26.01 | 14.36 | 1475.5 | 6.148 |
| D2H | 0.243 | 31.17 | 16.28 | 1632.9 | 6.718 |
| D3T | 0.245 | 24.50 | 15.40 | 1541.2 | 6.291 |
| D3S | 0.255 | 26.83 | 16.43 | 1648.5 | 6.465 |
| D3H | 0.260 | 33.87 | 17.42 | 1747.6 | 6.722 |

### 4.5 *Influence of Interaction Effect in Bi-tubes*

Each of the single polygonal tubes and single circular cylinder was compressed separately, and the summation of the mean crushing force was compared with the bi-tubular specimens in Table 7.

In D1T, D1S, and D1H, the clearance between the tubes is more. While crushing, the contact between the tubes is very less and both tubes are crushed almost separately. So the mean crushing force and the absorbed energy of D1T, D1S, and D1H bi-tubular specimens are approximately equal to the summation of their single tubes that is SC with S1T or S1S or S1H.

In D2T, D2S, and D2H, the clearance between the tubes is less compared to D1T, D1S, and D1H. While crushing, the contact between the tubes can cause the growth in mean crushing load and absorbed energy. So the mean crushing force of D2T, D2S, and D2H bi-tubular specimens are 7.3, 12.3, and 7.5% higher than the summation of their single tubes that is SC with S2T or S2S or S2H.

Like that, in D3T, D3S, and D3H the clearance between the tubes is very less compared to D1T, D1S, and D1H. While crushing the contact between the two tubes becomes tighter, it can cause the growth in mean crushing load. The mean crushing force of D3T, D3S, and D3H bi-tubular specimens is 35, 26, and 10.1% higher than the summation of their single tubes that is SC with S3T or S3S or S3H. Table 7 and Fig. 6 clearly show that the improvements of mean crushing force of bi-tubular specimens are increased with an inscribed diameter of inner tube.

**Table 7** Improvement of mean crushing force in bi-tubes

| Specimen code | | Experimental mean crushing force (kN) | | Improvement in $F_{\text{mean}}(\%)$ |
|---|---|---|---|---|
| Single tubes | Equivalent bi-tube | Summation of single tubes | Bi-tube | |
| SC + S1T | D1T | 8.18 + 2.81 = 10.99 | 10.76 | 2.1 |
| SC + S2T | D2T | 8.18 + 3.11 = 11.29 | 12.11 | 7.3 |
| SC + S3T | D3T | 8.18 + 3.25 = 11.43 | 15.4 | 35 |
| SC + S1S | D1S | 8.18 + 4.45 = 12.63 | 12.59 | 0.32 |
| SC + S2S | D2S | 8.18 + 4.62 = 12.8 | 14.36 | 12.3 |
| SC + S3S | D3S | 8.18 + 4.88 = 13.06 | 16.43 | 26 |
| SC + S1H | D1H | 8.18 + 6.1 = 14.28 | 14.57 | 2 |
| SC + S2H | D2H | 8.18 + 6.96 = 15.14 | 16.28 | 7.5 |
| SC + S3H | D3H | 8.18 + 7.55 = 16.73 | 17.42 | 10.1 |

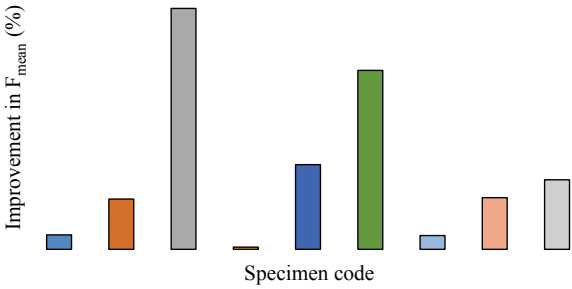


**Fig. 6** Effect of interaction on mean crushing force

## 5 Conclusions

In this research paper, the crashworthiness behavior of single thin-walled tubes with circular, triangular, square, and hexagonal sections was studied under quasi-static axial compression. From this experimental study, the following conclusion can be drawn:

1. In single tubes, the Total Energy Absorption (TEA) and mean crushing force ($F_{\text{mean}}$) are increased with increasing the inscribed diameter of polygonal section. $F_{\text{mean}}$ and Specific Energy Absorption (SEA) are increased with increasing the number of edges or corners of the section for any one of inscribed diameter of polygon.
2. Experimental mean crushing force of single tubes was compared with theoretical values and found that they have good consistency between them. Bi-tubular structures had greater SAE than the single tubes.
3. Effect of interaction or clearance between the tubes in bi-tubular arrangement was analyzed in detail. The mean crushing force of D1T, D1S, and D1H bi-tubular specimens is approximately equal to the summation of their single tubes that is SC with S1T or S1S or S1H.
4. In the second and third levels of inscribed diameter of inner tubes, the clearance between the tubes is minimum. Less clearance makes more interaction between the tubes, and it causes more energy absorption in bi-tubular arrangement. The mean crushing force for D3T was 35% greater than the summation of their single tubes that is SC with S3T. From this analysis, the interaction effect between the tubes is proved experimentally.

## References

1. Olabi AG, Morris E, Hashmi MSJ (2007) Metallic tube type energy absorbers: a synopsis. Thin-Walled Struct 46:706–726
2. Lu G, Yu T (2003) Energy absorption of structures and materials. Woodhead Publishing Ltd., Cambridge

3. Baroutaji A, Sajjia M, Olabi AG (2017) On the crashworthiness performance of thin-walled energy absorbers: Recent advances and future developments. Thin-Walled Struct 118:137–163
4. Fang J, Sun G, Qiu N, Kim NH, Li Q (2016) On design optimization for structural crashworthiness and its state of the art. Struct Multidisc Optim 55:1091–1119
5. Alexander JM (1960) An approximate analysis of the collapse of thin cylindrical shells under axial loading. Q J Mech Appl Math XIII:10–15
6. Abramowicz W, Jones N (1984) Dynamic axial crushing of circular tubes. Int J Impact Eng 2(3):263–281
7. Hong W, Jin FN, Zhou JN, Xia ZC, Xu Y, Yang L, Zheng Q, Fan H (2013) Quasi-static axial compression of triangular steel tubes. Thin Walled Struct 62:10–17
8. Abramowicz W, Wierzbicki T (1989) Axial crushing of multi corner sheet metal columns. J Appl Mech 56:113–120
9. Alavi Nia A, Hamedani JH (2010) Comparative analysis of energy absorption and deformations of thin walled tubes with various section geometries extrusions. Thin-Walled Struct 48:946–954
10. Alavi Nia A, Parsapour M (2014) Comparative analysis of energy absorption capacity of simple and multi-cell thin-walled tubes with triangular, square, hexagonal and octagonal sections. Thin-Walled Struct 74:155–165
11. Velmurugan R, Muralikannan R, Malhotra SK, Sudharsan V (2011) Energy absorption characteristics of dual phase steel tubes under static and dynamic loading. Strain 47:387–401
12. Velmurugan R, Muralikannan R (2009) Energy absorption characteristics of annealed steel tubes of various cross sections in static and dynamic loading. Lat Am J Solids Struct 6:385–412
13. Hanssen AG, Langseth M, Hopperstad OS (2000) Static and dynamic crushing of circular aluminium extrusions with aluminium foam filler. Int J Impact Eng 24(5):347–383
14. Hanssen AG, Langseth M, Hopperstad OS (1999) Static crushing of square aluminium extrusions with aluminium foam filler. Int J Mech Sci 41(8):967–993
15. Hanssen AG, Langseth M, Hopperstad OS (2001) Optimum design for energy absorption of square aluminium columns with aluminium foam filler. Int J Mech Sci 43(1):153–176
16. Hussein RD, Ruan D, Lu G, Guillow S, Yoon JW (2017) Crushing response of square aluminium tubes filled with polyurethane foam and aluminium honeycomb. Thin-Walled Struct 110:140–154
17. Yin H, Wen G, Hou S, Chen K (2011) Crushing analysis and multiobjective crashworthiness optimization of honeycomb-filled single and bi-tubular polygonal tubes. Mater Des 32:4449–4460
18. Gao Q, Wang L, Wang Y, Wang C (2016) Crushing analysis and multiobjective crashworthiness optimization of foam-filled ellipse tubes under oblique impact loading. Thin-Walled Struct 100:105–112
19. Sharifi S, Shakeri M, Ebrahimi Fakhari H, Bodaghi M (2015) Experimental investigation of bitubal circular energy absorbers under quasi-static axial load. Thin-Walled Struct 89:42–53
20. Vinayagar K, Senthil Kumar A (2017a) Multi-response optimization of crashworthiness parameters of bi-tubular structures. Steel Compos Struct 23(1):31–40
21. Haghi Kashani M, Shahsavari Alavijeh H, Akbarshahi H, Shakeri M (2013) Bitubular square tubes with different arrangements under quasi-static axial compression loading. Mater Des 51:1095–1103
22. Vinayagar K, Senthil Kumar A (2017b) Crashworthiness analysis of double section bi-tubular thin-walled structures. Thin-Walled Struct 112:184–193
23. Rahi A (2018) Controlling energy absorption capacity of combined bitubular tubes under axial loading. Thin-Walled Struct 123:222–231
24. Kamran M, Xue P, Ahmed N, Zahran MS, Hanif AG (2017) Axial crushing of uni-sectional bi-tubular inner tubes with multiple outer cross-sections. Lat Am J Solids Struct 14:2198–2220